Potential Fields Illuminate Geologic Factors Associated with Subduction-Margin Earthquakes

Richard J. Blakely and Ray E. Wells, U.S. Geological Survey, 345 Middlefield Rd, Menlo Park, CA 94025, USA

Abstract

Subduction zones generate three kinds of dangerous earthquakes. Megathrust earthquakes (M 8-9) occur along the thrust contact between the descending slab and overriding plate; intraslab earthquakes (M 7-8) occur within the descending slab as it passes through critical depths and undergoes important metamorphic changes; and crustal earthquakes (M 7-8) are generated by shallow faults in the overriding plate as the forearc responds to subduction-related stresses. The advent of new global compilations of gravity and magnetic anomaly data provides promise for understanding the geologic factors associated with each of these three types of hazardous earthquakes.

Megathrust Earthquakes

Megathrust earthquakes are the largest earthquakes in the world, as demonstrated by the 2004 M_W 9.0 earthquake at the Sumatra-Andaman Islands. Satellite free-air gravity anomalies over subduction zones often consist of an offshore trench-parallel gravity low and a sub parallel coastal gravity high reflecting the topography and structure of the inner trench slope and coast ranges, respectively (Wells et al., 2003; Song and Simons, 2003). Asperities (regions of greatest coseismic slip) in shallow megathrust earthquakes generally correlate with gravity lows centered on large forearc sedimentary basins along the offshore deep-sea terrace (Figure 1). The trench-parallel gravity low, the basins, and the earthquakes are all thought to be related to the resistance to slip along the plate boundary, and basin-centered gravity lows in similar settings may indicate the location of asperities in future megathrust earthquakes.

Intraslab Earthquakes

Landward of the shallow megathrust, magnetic anomalies provide clues to processes occurring within the subducting slab and overlying mantle wedge. In some subduction zones, water released from the transformation of basalt to eclogite in the descending slab hydrates overlying sub-continental mantle, produces serpentinite, embrittles the descending slab, and promotes intraslab earthquakes (Kirby et al., 2002). The 1970 central Peru earthquake (M_W 7.5 to 8.0) and the 1949 Olympia, Washington, earthquake (M_W 7.1) are recent examples.

Thermal models (e.g., Hyndman and Wang, 1995) indicate that the hydrated mantle wedge in most subduction zones is cooler than the Curie temperature of magnetite. If serpentinite is sufficiently abundant, hydrated mantle wedges will produce long-wavelength magnetic anomalies observable at the earth's surface. A crust-mantle model of the Cascadia subduction margin based on magnetic, gravity, and seismic data is consistent with the presence of significant volumes of hydrated mantle (Blakely et al., 2005). The advent of new global magnetic databases may allow us to map hydrated mantle worldwide. The World Digital Magnetic Anomaly

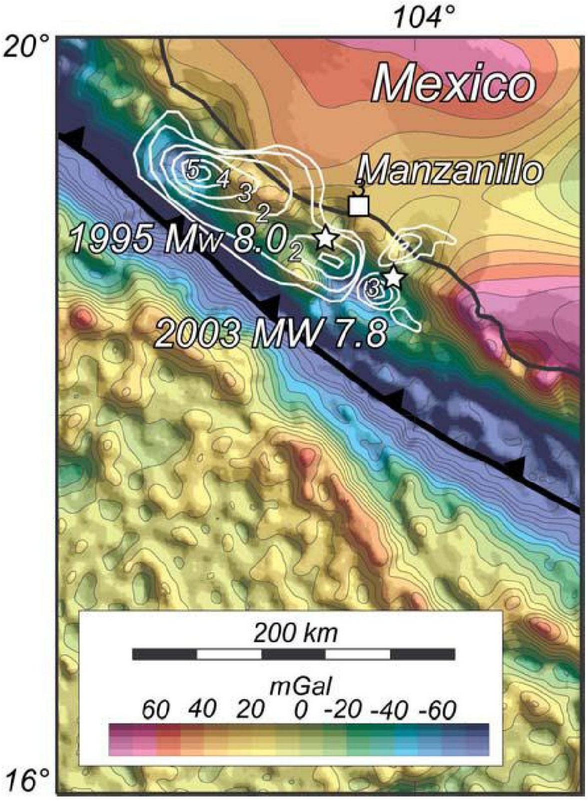

Figure 1. Free-air gravity anomalies, offshore northern Mexico. White contours are coseismic slip during the 1995 M_W 8.0 Jalisco earthquake (Schmitt et al., 2007) and the 2003 M_W 7.8 Colima earthquake (Yagi et al., 2004). Slip contours in m. Note that greatest slip during those earthquakes occurred within a forearc sedimentary basin reflected in free-air gravity anomalies.

Map and the CHAMP satellite magnetic field, processed to emphasize sources at mantle depths, show evidence for hydrated mantle at many subduction margins of the world, including Cascadia, northeast Japan, the Aleutians, southern Mexico, and Central America (Figure 2). All of these subduction zones have thermal characteristics believed to be conducive for intraslab earthquakes. On the other hand, the Nankai, Peru, and Chile subduction margins, also known to be susceptible to intraslab earthquakes, have only minor forearc magnetic anomalies, indicating complexities in the relationship between hydrated mantle and intraslab seismogenesis.

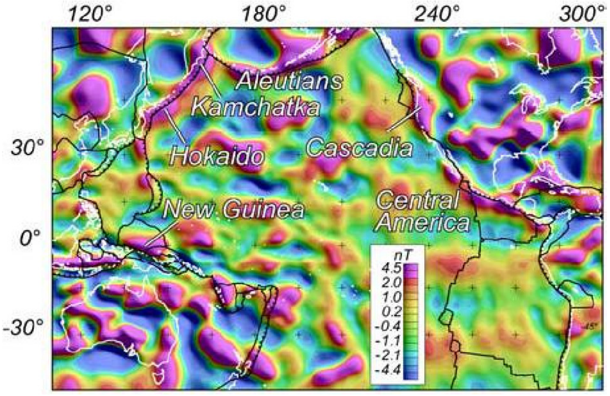

Figure 2. CHAMP satellite magnetic anomaly data (Maus et al., 2007) at 350 km altitude. Large magnetic anomalies are evident over forearc regions, notably the Aleutians, Kamchatka, Hokaido, New Guinea, Central America, and Cascadia.

Crustal Earthquakes

In the shallow crust of the subduction-margin forearc, magnetic fields illuminate active faults triggered by stresses induced by the subducting plate. The Seattle fault, source of a M_W 7.5 earthquake 1100 ka, and the Nojima Fault, source of the M_W 6.9 Kobe earthquake in 1995, are well-known examples from Cascadia and Nankai, respectively. In Cascadia, where bedrock is commonly concealed by vegetation and young glacial deposits, potential-field mapping is integrated with laser terrain mapping (lidar), which reveals scarps cutting late-Pleistocene glacial surfaces (e.g., Sherrod at al., 2008; Blakely et al., in review; Figure 3). In almost every case, these lidar scarps correspond with short-wavelength, low-amplitude magnetic anomalies in high-resolution aeromagnetic surveys, which in turn facilitate geologic mapping of the faults away from scarps and help to characterize faults at depth. The lidar and aeromagnetic data together provide targets for follow-on trench excavations that yield temporal information on past earthquakes needed to assess earthquake hazards.

Summary and Conclusions

Global compilations of gravity (e.g., Smith and Sandwell, 1997) and magnetic (e.g., Hemant et al., 2007; Maus et al., 2007) anomaly data provide new opportunities for understanding the geologic factors associated with hazardous earthquakes in subduction-margin settings around the world. Free-air gravity anomalies over the trench slope reflect structural basins kinematically linked with known regions of greatest slip during past great earthquakes, and may provide a means to predict regions of greatest slip in future great earthquakes. Magnetic anomalies over forearc regions have long-wavelength components caused by hydrated mantle. In some subduction zones, hydrated mantle is expected to be spatially associated with intraslab earthquakes. Combined interpretation of lidar and magnetic anomaly surveys, with follow-on paleoseismic investigations, permit mapping of concealed, active crustal faults at regional scales and with unprecedented accuracy. The U.S. Geological Survey, along with many other organizations, is actively engaged in all of these research endeavors.

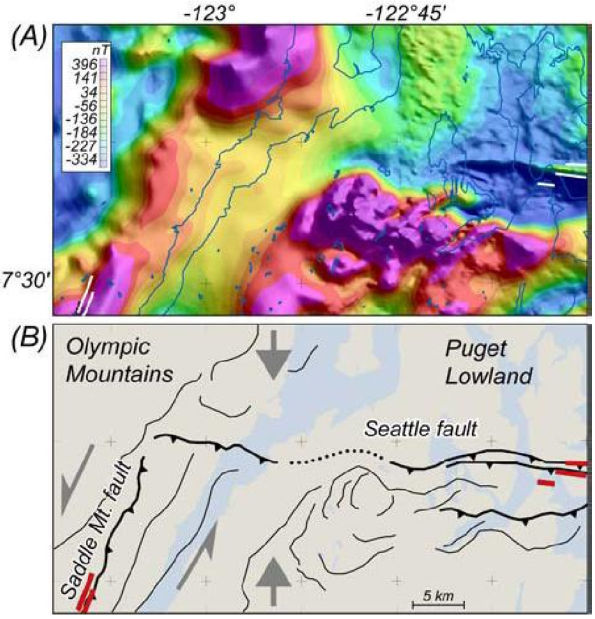

Figure 3. Interpretation of high-resolution aeromagnetic anomalies from the Olympic Peninsula, Washington. (A) Aeromagnetic anomalies shown as rainbow colors. White lines are topographic scarps mapped from lidar data (B) Interpretation of concealed faults. Red lines are lidar scarps. Gray arrows indicate inferred strain directions.

References

Blakely, R.J., Brocher, T.M., and Wells, R.E., 2005, Subduction-zone magnetic anomalies and implications for hydrated forearc mantle: Geology, v. 33, p. 445-448.

Blakely, R.J., Sherrod, B.L., Hughes, J.F., Anderson, M.L., Wells, R.E., and Weaver, C.S., 2008, The Saddle Mountain fault, Olympic Peninsula, Washington: Western Boundary of the Seattle uplift?: Geosphere, in review.

Blakely, R.J., Wells, R.E., Weaver, C.S., and Johnson, S.Y., 2002, Location, structure, and seismicity of the Seattle fault zone, Washington: Evidence from aeromagnetic anomalies, geologic mapping, and seismic-reflection data: Geological Society of America Bulletin, v. 114, p. 169-177.

Hemant, K., Thebault, E., Mandea, M., Ravat, D., and Maus, S., 2007, Magnetic anomaly map of the world; merging satellite, airborne, marine, and ground-based magnetic data sets: Earth and Planetary Science Letters, v. 260, p. 56-71.

Hyndman, R.D., and Wang, K., 1995, The rupture zone of Cascadia great earthquakes from current deformation and the thermal regime: Journal of Geophysical Research, v. 100, p. 22,133-22,154.

Kirby, S.H., Engdahl, E.R., and Villasenor, A., 2002, Warm-slab subduction as a global process, in The Cascadia Subduction Zone and Related Subduction Systems, edited by Kirby, S.H., Wang, K., and Dunlop, S.G., p. 75, U.S. Geological Survey Open-File Report 02-328, Geological Survey of Canada Open File 4350.

Maus, S., Luehr, H., Rother, M., Hemant, K., Balasis, G., Ritter, P., and Stolle, C., 2007, Fifth-generation lithospheric magnetic field model from CHAMP satellite measurements: Geochemistry, Geophysics, Geosystems, v. 8, no. 5, Q05013.

Schmitt, S.V., DeMets, C., Stock, J., Sanchez, O., Marquez-Azua, B., and Reyes, G., 2007, A geodetic study of the 2003 January 22 Tecoman, Colima, Mexico earthquake: Geophysical Journal International, v. 169, p. 389-406.

Sherrod, B.L., Blakely, R.J., Weaver, C.S., Kelsey, H.M., Barnett, E., Liberty, L., Meagher, K.L., and Pape, K., 2008, Finding concealed active faults: Extending the southern Whidbey Island fault across the Puget Lowland, Washington: Journal of Geophysical Research, v. 113, B05313, doi:10.1029/2007JB005060, 25 p.

Smith, W., and Sandwell, D.T., 1997, Gobal sea foor topography from satellite altimetry and ship depth soundings: Science, v. 277, no. 5334, p. 1956-1962.

Song, T.A., and Simons, M., 2003, Large trench-parallel gravity variations predict seismogenic behavior in subduction zones: Science, v. 301, p. 630-633.

Wells, R.E., Blakely, R.J., Sugiyama, Y., Scholl, D.W., and Dinterman, P.A., 2003, Basin-centered asperities in great subduction zone earthquakes: A link between slip, subsidence, and subduction erosion?: Journal of Geophysical Research, v. 108, no. B10, 2507, doi:10.1029/2002JB002072.

Yagi, Y., Mikumo, T., and Pacheco, J., and Reyes, G., 2004, Source rupture process of the Tecoman, Colima, Mexico earthquake of 22 January 22 2003, determined by joint inversion of teleseismic body-wave and near-source data: Bulletin of the Seismological Society of America, v. 94, p. 1795-1807.